Roles of IP$_3$R and RyR Ca^{2+} Channels in Endoplasmic Reticulum Stress and β-Cell Death

Dan S. Luciani, Kamila S. Gwiazda, Ting-Lin B. Yang, Tatyana B. Kalynyak, Yaryna Bychkivska, Matthew H.Z. Frey, Kristin D. Jeffrey, Arthur V. Sampaio, T. Michael Underhill, and James D. Johnson

OBJECTIVE—Endoplasmic reticulum (ER) stress has been implicated in the pathogenesis of diabetes, but the roles of specific ER Ca^{2+} release channels in the ER stress–associated apoptosis pathway remain unknown. Here, we examined the effects of stimulating or inhibiting the ER-resident inositol trisphosphate receptors (IP$_3$Rs) and the ryanodine receptors (RyRs) on the induction of β-cell ER stress and apoptosis.

RESEARCH DESIGN AND METHODS—Kinetics of β-cell death were tracked by imaging propidium iodide incorporation and caspase-3 activity in real time. ER stress and apoptosis were assessed by Western blot. Mitochondrial membrane potential was monitored by flow cytometry. Cytosolic Ca^{2+} was imaged using fura-2, and genetically encoded fluorescence resonance energy transfer (FRET)–based probes were used to measure Ca^{2+} in ER and mitochondria.

RESULTS—Neither RyR nor IP$_3$R inhibition, alone or in combination, caused robust death within 24 h. In contrast, blocking sarco/endoplasmic reticulum ATPase (SERCA) pumps depleted ER Ca^{2+} and induced marked phosphorylation of PKR-like ER kinase (PERK) and eukaryotic initiation factor-2α (eIF2α), C/EBP homologous protein (CHOP)–associated ER stress, caspase-3 activation, and death. Notably, ER stress following SERCA inhibition was attenuated by blocking IP$_3$Rs and RyRs. Conversely, stimulation of ER Ca^{2+} release channels accelerated thapsigargin-induced ER depletion and apoptosis. SERCA block also activated caspase-9 and induced perturbations of the mitochondrial membrane potential, resulting eventually in the loss of mitochondrial polarization.

CONCLUSIONS—This study demonstrates that the activity of ER Ca^{2+} channels regulates the susceptibility of β-cells to ER stress resulting from impaired SERCA function. Our results also suggest the involvement of mitochondria in β-cell apoptosis associated with dysfunctional β-cell ER Ca^{2+} homeostasis and ER stress. *Diabetes* 58:422–432, 2009

Inappropriate activation of cell death pathways in the pancreatic β-cell is involved in the pathogenesis of type 1 diabetes, type 2 diabetes, and rare diabetic disorders such as maturity-onset diabetes of the young, Wolcott-Rallison syndrome, and Wolfram syndrome (1–5). β-Cell apoptosis also hampers clinical islet transplantation (6). The endoplasmic reticulum (ER) plays a key role in multiple programmed cell death pathways (7–9). Apoptosis caused by ER stress has been associated with diabetes (1,2,5,10) and can be induced by the accumulation of unfolded proteins resulting from disrupted Ca^{2+}-dependent chaperone function in the ER (1,11). Both thapsigargin, a potent and specific inhibitor of sarco/endoplasmic reticulum ATPase (SERCA), and endogenous factors that downregulate SERCA, evoke ER stress and apoptosis in β-cells (12,13). However, the detailed mechanisms underlying Ca^{2+}-dependent apoptosis and the roles played by specific β-cell ER Ca^{2+} channels and pumps in ER stress remain unclear.

In addition to multiple SERCA isoforms (14), the β-cell ER expresses several classes of intracellular Ca^{2+}-releasing channels, including the inositol trisphosphate receptors (IP$_3$Rs) and the ryanodine receptors (RyRs) (15–19). In the diabetic state, the expression of these receptors is known to be modulated in several cell types, including β-cells (15,20–22). We have previously shown that long-term inhibition of RyR2 in low glucose leads to programmed β-cell death involving calpain-10, but not caspase-3; conversely, RyR inhibition protected islets under conditions of chronic hyperglycemia (17). We have also shown that RyR inhibition significantly reduces the ratio of ATP to ADP in MIN6 β-cells (23), an event that could conceivably activate ER stress (24,25). Furthermore, studies of other cells types have suggested that ER stress–associated damage can be affected by inhibitors of RyRs (26) or IP$_3$Rs (27). Despite these important questions and links, studies on the roles of RyRs and IP$_3$Rs in β-cell ER stress have not been published to date.

In the present study, we investigated whether disrupting β-cell ER Ca^{2+} homeostasis by blocking Ca^{2+} release through IP$_3$Rs and RyRs is sufficient to induce ER stress. We also tested the hypothesis that stimulating or inhibiting these channels would alter ER stress or apoptosis triggered by ER Ca^{2+} depletion following SERCA inhibition. Our results demonstrate that while blocking ER Ca^{2+} release channels does not induce a major ER stress response, Ca^{2+} flux from both RyRs and IP$_3$Rs can modulate β-cell apoptosis and ER stress resulting from impaired SERCA function.
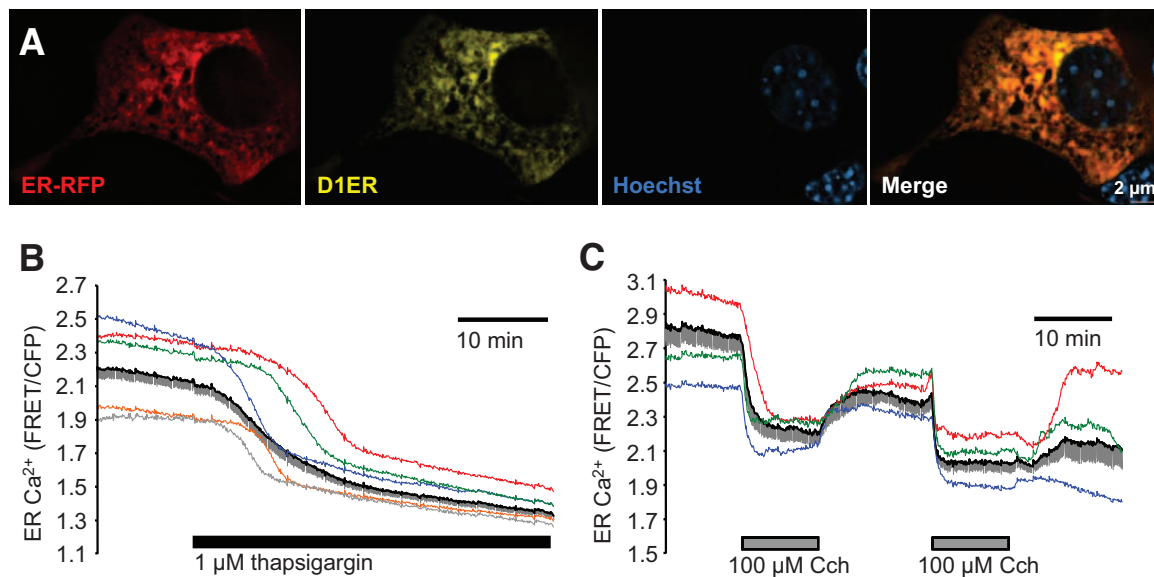
FIG. 1. ER Ca²⁺ dynamics during acute SERCA inhibition and IP₃R activation in MIN6 β-cells. *A*: Subcellular colocalization of mRFP targeted to the ER using the KDEL protein sequence and DIER cameleon in transfected MIN6 cells. *B*: A total of 1 μmol/l thapsigargin evoked a gradual depletion of luminal ER Ca²⁺. An average trace is shown in black ($n = 14$ cells), and profiles from individual cells are shown to illustrate the response heterogeneity. *C*: Repeatable and reversible lowering of ER luminal Ca²⁺ due to IP₃R activation by successive carbachol (Cch) treatments as indicated. An average response is shown in the black trace ($n = 9$ cells) along with representative single cell traces. (Please see http://dx.doi.org/10.2337/db07-1762 for a high-quality digital representation of this figure.)

RESEARCH DESIGN AND METHODS

Cell culture and transfection. MIN6 cells were cultured and transfected as described previously (23). Cells were imaged 48–72 h after transfection. Pancreatic islets were obtained from 8- to 16-week-old male C57BL6/J mice by collagenase digestion and filtration and cultured as described (28,29). For high-throughput imaging–based cell death assays, islets were hand-picked the next day and dispersed into single cells and plated on 96-well plates (see below).

Reagents. Thapsigargin (Tg) was purchased from Calbiochem (La Jolla, CA) or Sigma (St. Louis, MO) and was kept as a 1,000× DMSO stock. Tetramethylrhodamine ethyl ester perchlorate (TMRE) (Sigma), xestospongin C (AG Scientific, San Diego, CA; Calbiochem), ryanodine (Molecular Probes, Eugene, OR; Tocris, Ellisville, MO; Calbiochem), dantrolene, CGP-37157, and carbonyl cyanide *m*-chlorophenyl-hydrazone (CCCP) (Calbiochem) were dissolved in DMSO. Carbachol from Calbiochem was dissolved in water.

Single-cell imaging. Single-cell imaging was performed in Ringer's solution containing (in mmol/l): 5.5 KCl, 2 CaCl₂, 1 MgCl₂, 20 HEPES, 141 NaCl, and 3 glucose. Cytosolic Ca²⁺ was imaged in fura-2-AM–loaded cells as described previously (4,30). Preheated solutions were applied by stable perifusion at 1 ml/min, and complete solution changes were achieved in <30 s.

ER luminal and mitochondrial Ca²⁺ was imaged using the fluorescence resonance energy transfer (FRET)-based D1ER and mt4D3cpv cameleons, respectively (31,32). The cyan fluorescent protein (CFP) component of the probes was excited using a S430/25x filter (Chroma). CFP and FRET (i.e., yellow fluorescent protein) emission were alternately collected using S470/30m and S535/30m filters mounted in a Sutter Lambda 10-2 filter wheel. Changes in ER and mitochondrial Ca²⁺ were expressed as the FRET-to-CFP emission ratio. There was no correlation between the apparent Ca²⁺ levels and the intensity of the FRET probe in the cells used for this study.

Single-cell, FRET-based imaging of caspase-3 activity was performed using the MiCy-DEVD-mKO probe (33). Activation of caspase-3 cleaves this probe and results in a loss of FRET between a CFP (MiCy) and an orange fluorescent protein (mKO). MiCy excitation and emission was controlled by 436/20x and 490/40m filters, respectively. FRET with mKO was measured using a 585/60m filter and normalized to MiCy emission intensity.

High-throughput imaging of cell death kinetics. For kinetic analysis of cell death, MIN6 cells or dispersed mouse islet cells were plated onto glass-bottom 96-well microplates (ViewPlate-96; Perkin Elmer) in culture media (see above) and treated as indicated. Cell death was monitored by the incorporation of propidium iodide (PI) (250–500 ng/ml in each well). PI fluoresces brightly only once it passes through the compromised plasma membrane and binds to DNA. It labels cells in the last stages of apoptosis that follow caspase activation, as well as cells undergoing necrosis (34). Approximately 30 min after treatment, 96-well plates were imaged at 37°C and 5% CO₂ using a Cellomics KineticScan (Pittsburgh, PA). Two to four nonoverlapping images were taken from each well at 30- or 60-min intervals. PI-positive cells were automatically identified and counted using the Target Activation Bioapplication (Cellomics, Pittsburgh, PA). Cell death is presented as an absolute count of PI-positive cells and quantified by calculating the incremental area under the curve. Plots of representative cell death profiles show the means ± SE of three independent cultures imaged simultaneously. For statistical comparisons, we used a conservative approach in which the average response of three similarly treated, independent cell cultures on a microplate was treated as a separate "*n*". At least three of these replicate sets were performed on separate days for each study.

Flow cytometry analysis of mitochondrial membrane potential. Changes in mitochondrial membrane potential were estimated by flow cytometry of MIN6 cells stained with TMRE (35). After the indicated treatments, all floating and adherent cells were collected, spun down at 500*g* for 10 min, and loaded with 50 nmol/l TMRE in PBS with 2% fetal bovine serum (FBS) for 30 min at 37°C. The cells were washed again and kept in PBS for ~30 min before a total of 10⁵ events were collected using the FL2 channel of a Becton Dickinson FACScan. Cellular debris was identified by forward- and side-scatter criteria and excluded from analysis. Every set of measurements included a depolarized control sample pretreated for 30 min with 10 μmol/l of the mitochondrial uncoupler CCCP.

Immunoblotting. Western blots were carried out as described (23). Rabbit monoclonal antibody to cleaved caspase-3 was from Cell Signaling (Danvers, MA). Rabbit polyclonal anti–C/EBP homologous protein (CHOP) antibody was from Santa Cruz (Santa Cruz, CA). Rabbit monoclonal antibody to phospho–PKR-like ER kinase (PERK) and rabbit polyclonal antibody to phospho–eukaryotic initiation factor-2α (eIF2α) were from Cell Signaling. The antibody to total eIF2α was a mouse monoclonal from Abcam (Cambridge, MA). After three washes, membranes were incubated with secondary antibodies diluted in I-block (caspase-3, CHOP) or 5% BSA (PERK, eIF2α) for 1 h. In the case of phospho-PERK and phospho-eIF2α (detection), phosphatase inhibitor (Calbiochem) was added to the lysis buffer. After three washes with 0.1% Tween-PBS, immunoreactivity was visualized using chemiluminescence. Densitometric analysis was performed using Photoshop (Adobe Systems, San Jose, CA).

Data analysis. Unless otherwise indicated, data are presented as means ± SE. Differences between means were evaluated using Student's *t* test and were considered significant if $P < 0.05$.

RESULTS

Cytosolic and ER Ca²⁺ signals evoked by SERCA inhibition and IP₃R activation. The ER is involved in the regulation of multiple cell death pathways (7–9).
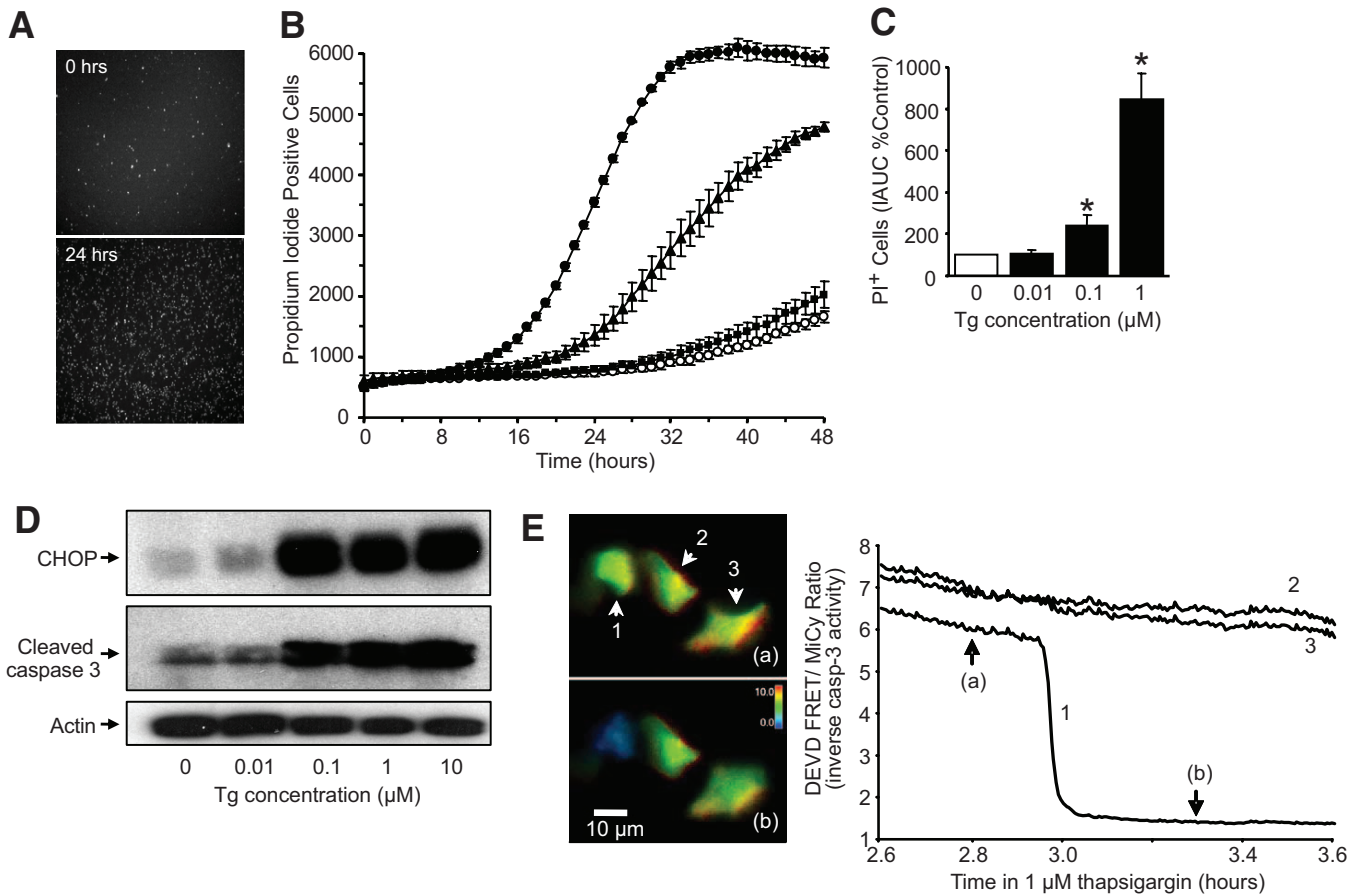
FIG. 2. Dose- and time-dependent effects of SERCA inhibition on CHOP expression, caspase-3 activation, and cell death. Cell death was assayed in real-time by propidium iodide incorporation in MIN6 cells. *A*: Images illustrating the progressive propidium iodide incorporation in a field of MIN6 cells exposed to 1 μmol/l thapsigargin (Tg). *B*: Representative time course of cell death in response to various concentrations of thapsigargin. ○, Control; ■, 0.01 μmol/l thapsigargin; ▲, 0.1 μmol/l thapsigargin; ●, 1 μmol/l thapsigargin. *C*: Dose dependence of the thapsigargin-induced MIN6 cell death, quantified as the area under the curves (IAUC) of the first 24 h of the propidium iodide incorporation profiles ($n = 3$). *D*: Induction of CHOP (~31-kDa band) and cleaved caspase-3 (~17- to 19-kDa band) in MIN6 cells cultured for 24 h in DMEM containing 25 mmol/l glucose and increasing concentrations of thapsigargin ($n = 3$). *E*: Representative real-time imaging of caspase-3 activation in living MIN6 cells using the MiCy-DEVD-mKO FRET probe. The loss of FRET/MiCy intensity ratio, observed in the cell marked as number one, between the time points marked (a) and (b), results from cleavage of the DEVD caspase-3 target sequence. The cells were imaged for a period of 5 h, during which caspase-3 was activated in 5 of 16 (31%) thapsigargin-treated cells and in 1 of 10 (10%) control cells. (Please see http://dx.doi.org/10.2337/db07-1762 for a high-quality digital representation of this figure.)

Although luminal ER Ca^{2+} levels are thought to play critical roles in many apoptotic cascades, measurements of Ca^{2+} dynamics within the ER under pro- and antiapoptotic conditions have remained technically challenging. Using fura-2 and FRET-based imaging, respectively, we measured the changes in cytosolic and ER luminal Ca^{2+} caused by inhibition of SERCA pumps and activation of IP$_3$Rs. Thapsigargin is a specific SERCA inhibitor known to induce apoptosis in many cell types including β-cells (12). In agreement with other studies (36), blocking ER Ca^{2+} uptake with thapsigargin evoked transient cytosolic Ca^{2+} rises in MIN6 β-cells, although not in every cell (data not shown). This suggests that there is a substantial steady-state leak from the ER or that SERCA pumps are a component of a critical Ca^{2+} buffering system in MIN6 cells. In agreement with other reports (12,37), we also confirmed that carbachol, a cholinergic agonist that causes IP$_3$ formation, rapidly mobilized intracellular Ca^{2+} to evoke a cytosolic Ca^{2+} peak in MIN6 and primary β-cells (data not shown). The initial Ca^{2+} spike was often followed by a lower, but sustained, Ca^{2+} elevation that depended on extracellular Ca^{2+} influx, suggesting a possible role for a Ca^{2+} release–activated Ca^{2+} current (i.e., CRAC channel) (38,39).

To extend these findings, we analyzed the dynamics of luminal ER Ca^{2+} directly by using the D1ER cameleon. This probe has an optimal sensitivity range, excellent signal-to-noise characteristics (31,32), and was designed to mitigate interference with endogenous Ca^{2+} signaling and reduce pH-based artifacts (31). D1ER was localized to the ER by virtue of both KDEL and calreticulin sequences and was observed in a reticular pattern that matches ER-targeted monomeric red fluorescent protein (Fig. 1*A*). Direct measurements of luminal Ca^{2+} demonstrated that treatment with 1 μmol/l thapsigargin resulted in a robust decrease in ER Ca^{2+} (Fig. 1*B*) and that carbachol stimulated Ca^{2+} release from the ER in a reversible and repeatable manner (Fig. 1*C*). Notably, the thapsigargin-induced lowering of ER Ca^{2+} was more gradual and characterized by larger cellular heterogeneity than that evoked by carbachol (Fig. 1*B* and *C*). In some cells, ER Ca^{2+} levels fell immediately upon SERCA inhibition, whereas a significant delay was seen in others, suggesting cell-to-cell differences in basal ER Ca^{2+} release rates (i.e., leak). Similar results were seen with 20 μmol/l 2,5-Di-(*t*-butyl)-1,4-hydroquinone, a structurally distinct SERCA inhibitor (data not shown). Together, these experiments validate the use of the D1ER cameleon in β-cells and demonstrate the dynam-
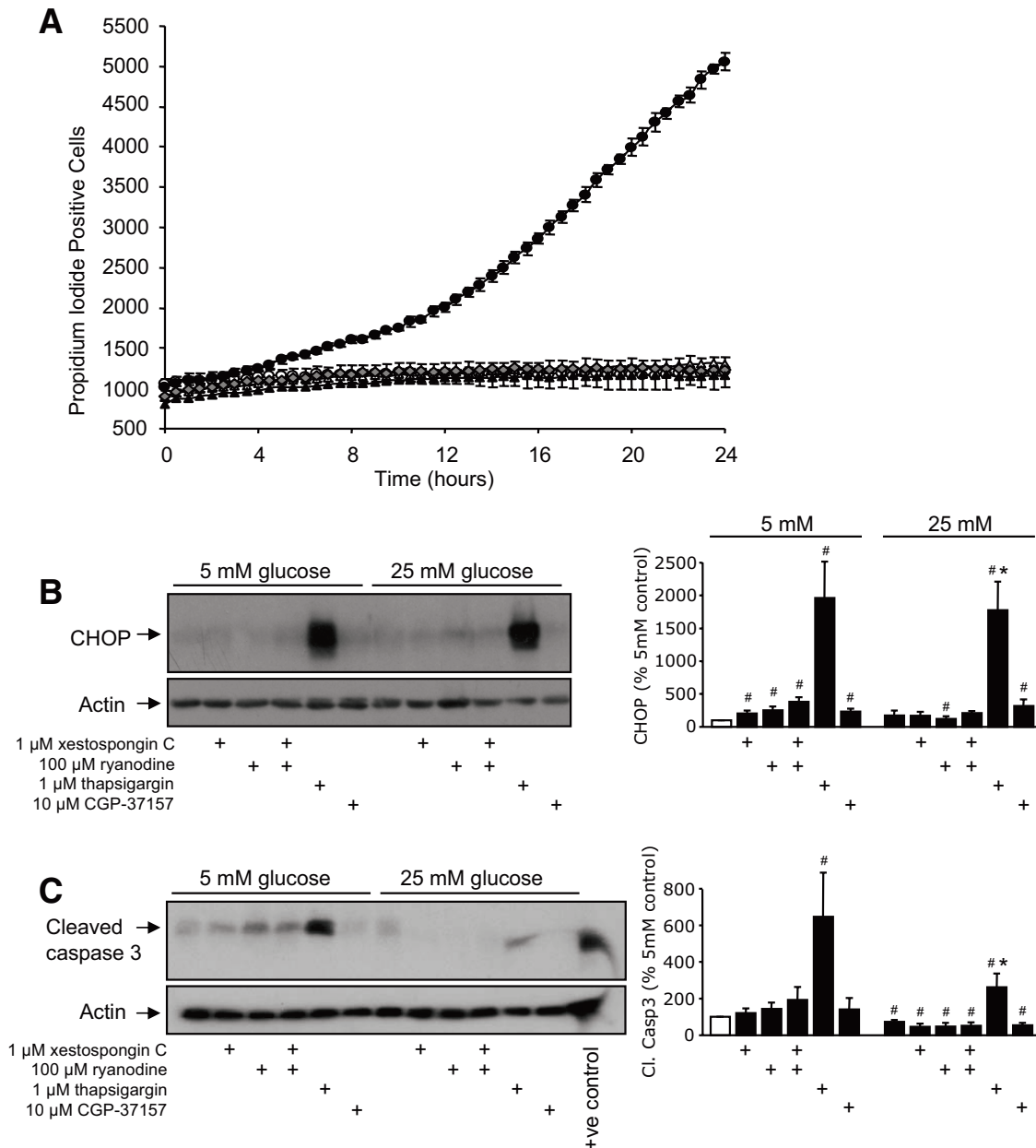
FIG. 3. ER stress and caspase-3–dependent cell death is induced by blocking Ca^{2+} pumps but not ER Ca^{2+} release channels. A: MIN6 cell death was monitored over 24 h in response to inhibition of RyR (100 μmol/l ryanodine), IP$_3$R (1 μmol/l xestospongin C), combined inhibition of RyR and IP$_3$R, or inhibition of SERCA pumps (1 μmol/l thapsigargin). All inhibitors were applied in culture media containing 25 mmol/l glucose. Traces are representative of six independent experiments. ○, control; △, 100 μmol/l ryanodine; ▲, 1 μmol/l xestospongin C; ◆, 100 μmol/l ryanodine + 1 μmol/l xestaspongin C; ●, 1 μmol/l thapsigargin. B: MIN6 cells were cultured as indicated and probed for markers of ER stress and apoptosis, as in Fig. 2. CHOP expression was examined and quantified at both low and high glucose ($n = 4$–10). C: Cleaved caspase-3 expression examined and quantified at both low and high glucose ($n = 4$–10). A positive control for cleaved (Cl.) caspase-3 supplied by the manufacturer (lysates from apoptotic T-cells) was included in the final lane. #$P < 0.05$ vs. 5 mmol/l glucose control; *$P < 0.05$ vs. 25 mmol/l glucose control.

ics of ER Ca^{2+} emptying when ER Ca^{2+} release channels are activated and ER Ca^{2+} uptake blocked, respectively.

Differential effects of blocking ER influx versus efflux on ER stress and apoptosis. ER Ca^{2+} homeostasis is regulated by both pumps and channels (19). To analyze the time course of cell death in response to blockers of β-cell Ca^{2+} pumps and channels, we utilized a high-throughput imaging platform to monitor propidium iodide incorporation for 24–48 h under normal incubated culture conditions. Both the time course and the degree of cell death were dose dependent in thapsigargin-treated cells (Fig. 2A–C). Cell death was associated with induction of ER stress, as demonstrated by increased expression of the transcription factor CHOP/GADD153 (Fig. 2D), an

essential component of ER stress–mediated apoptosis in β-cells (40). Western blotting also demonstrated that blocking ER Ca^{2+} pumps with thapsigargin activated caspase-3 (Fig. 2D) and increased cleaved caspase-7 by sixfold at 24 h ($P < 0.05$, $n = 4$; data not shown). We then used real-time single-cell FRET-based imaging to examine the dynamics of this process. Caspase-3–dependent loss of FRET was observed 2–4 h following the addition of thapsigargin (Fig. 2E). Hence, apoptosis of MIN6 cells is triggered relatively quickly following SERCA inhibition. Cyclopiazonic acid and 2-aminoethoxydiphenyl borate, two structurally distinct SERCA blockers (19,41), similarly induced β-cell ER stress and apoptosis (data not shown). These observations strongly suggest that thapsigargin trig-
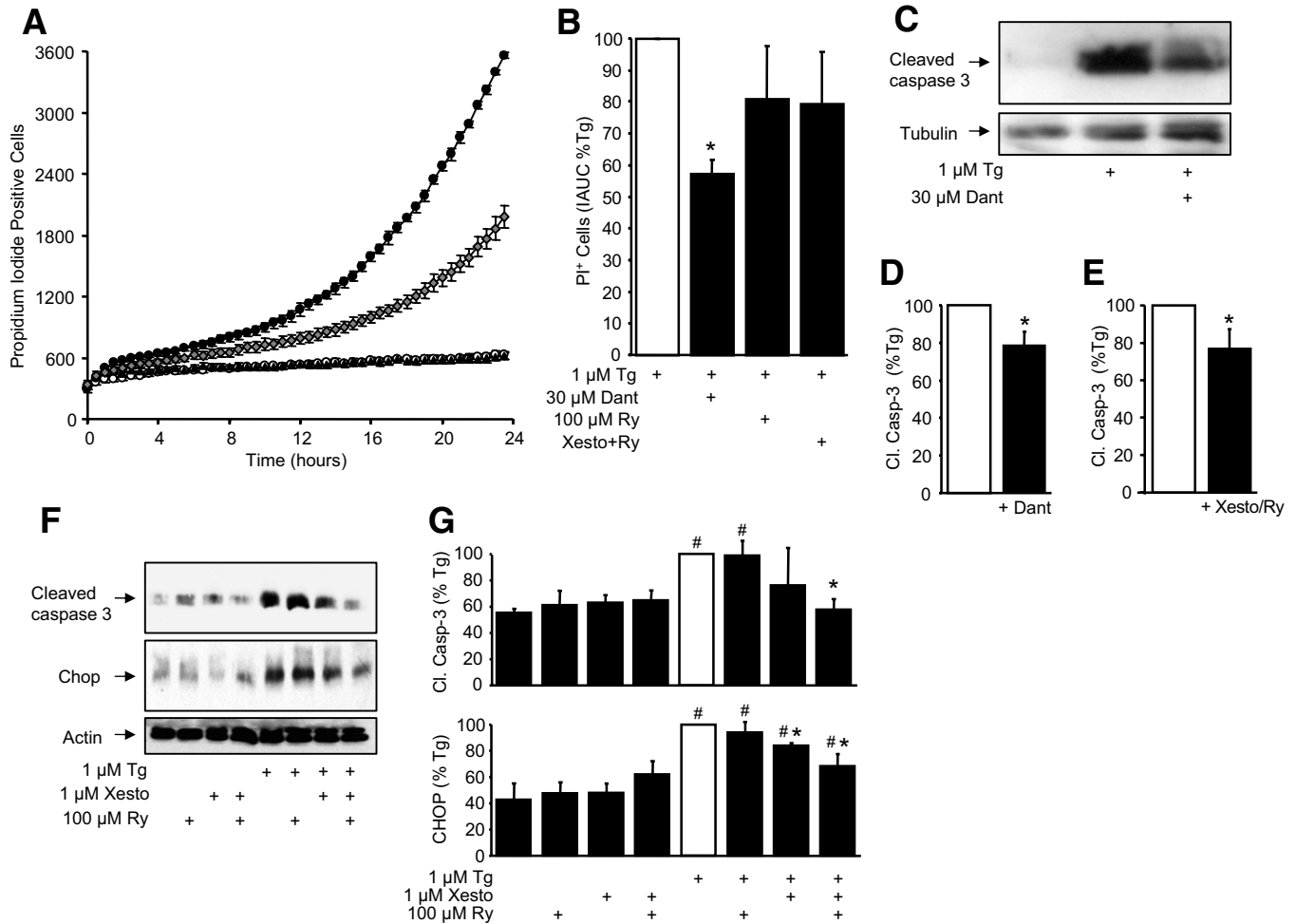
FIG. 4. ER Ca²⁺ channel blockers can reduce ER stress and apoptosis induced by thapsigargin (Tg). *A* and *B*: Cell death induced by 1 μmol/l thapsigargin was significantly attenuated by 30 μmol/l of the RyR1 inhibitor dantrolene (*n* = 4). *A*: ○, control; ▲, 30 μmol/l dantrolene; ●, 1 μmol/l thapsigargin; ◆, 1 μmol/l thapsigargin + 30 μmol/l dantrolene. A trend toward protection from thapsigargin-induced death was also observed in response to treatment with 100 μmol/l ryanodine alone (*n* = 4) or in combination with 1 μmol/l xestospongin C (*n* = 6). *C* and *D*: Caspase-3 activation following an 8-h treatment with thapsigargin was reduced by dantrolene (*n* = 3). *E*: Caspase-3 cleavage in MIN6 cells cultured at 5 mmol/l glucose for 24 h with 1 μmol/l thapsigargin in the presence or absence of both 100 μmol/l ryanodine and 1 μmol/l xestospongin C (*n* = 6). *F* and *G*: Quantified Western blots of cleaved caspase-3 and CHOP levels in MIN6 cells treated for 8 h in 5 mmol/l glucose as indicated (*n* = 3). #*P* < 0.05 vs. control; **P* < 0.05 vs. thapsigargin alone.

gered the ER stress response by specific inhibition of SERCA and provide a detailed kinetic analysis of β-cell apoptosis caused by ER stress.

We next investigated whether ER stress and apoptosis might be induced when ER-resident Ca²⁺ release channels (i.e., IP₃Rs and RyRs) are blocked under conditions of normal ER Ca²⁺ uptake. Inhibition of RyRs for 24 h with 100 μmol/l ryanodine did not induce death in MIN6 cells cultured in high glucose (Fig. 3*A*), in agreement with our previous findings (17). When compared with thapsigargin, ryanodine did not evoke a similarly robust increase in CHOP expression or caspase-3 cleavage (Fig. 3), although preliminary analysis indicated that calpain-10 protein levels were upregulated (not shown), consistent with our previous results (17,23). We also utilized the IP₃R inhibitor, xestospongin C, previously demonstrated to block IP₃-dependent Ca²⁺ release in pancreatic β-cells (42,43). As was the case with ryanodine, the effects of 1 μmol/l xestospongin C on CHOP, caspase-3, and cell death were modest. Simultaneous inhibition of RyRs and IP₃Rs also did not cause cell death, ruling out the possibility of compensatory Ca²⁺ flux through one class of channel when the other type was blocked (Fig. 3). CGP-37157, a

drug that has been reported to indirectly interfere with ER Ca²⁺ uptake by blocking mitochondrial Na⁺/Ca²⁺ exchange (30,44), had little effect on ER stress or caspase-3 activation. It should be noted, however, that we have previously demonstrated that CGP-37157 also inhibits voltage-gated Ca²⁺ entry in β-cells (30). There was a tendency for caspase-3 cleavage to be reduced by changing the glucose concentration from 5 to 25 mmol/l (Fig. 3*B* and *C*). Together, these experiments demonstrated that marked ER stress and caspase-3–dependent apoptosis were induced specifically by inhibition of ER Ca²⁺ uptake but not by inhibition of ER Ca²⁺ release via RyR and IP₃R channels. **IP₃Rs and RyRs participate in ER stress and apoptosis caused by SERCA inhibition.** The level of Ca²⁺ in the ER lumen reflects the balance between influx and efflux. We sought to establish the role of channel-mediated efflux in β-cell ER stress and apoptosis. First, we tested the hypothesis that reducing ER Ca²⁺ release might ameliorate the effects of thapsigargin. Indeed, the RyR blocker dantrolene protected MIN6 cells from thapsigargin-induced death (Fig. 4*A* and *B*). Ryanodine (100 μmol/l), alone or in combination with xestospongin C (1 μmol/l), also suppressed thapsigargin-induced pro-
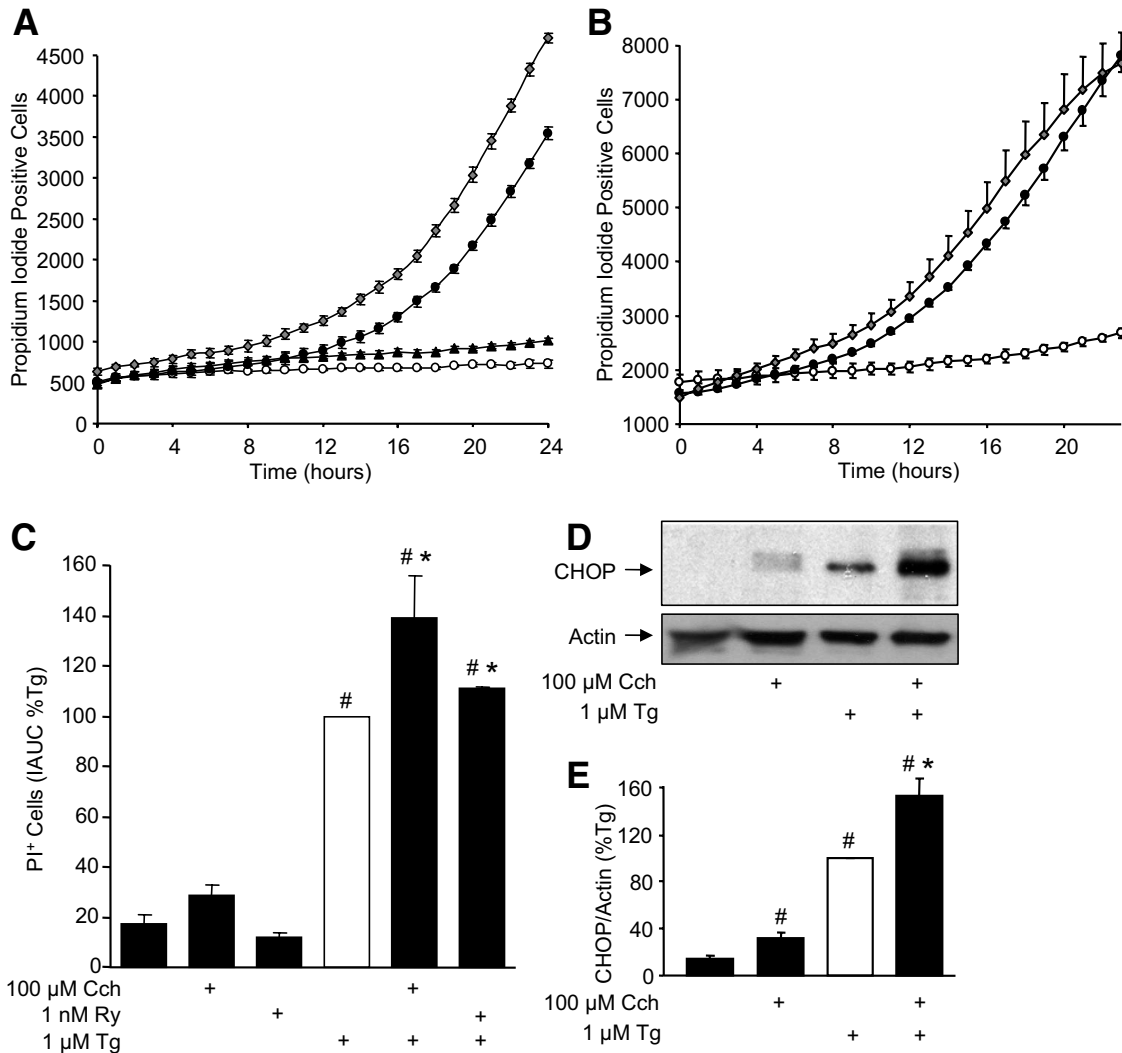
FIG. 5. IP$_3$ and ryanodine receptor activation augments β-cell death and ER stress. A–C: Cholinergic activation of IP$_3$R by 100 μmol/l carbachol (Cch; $n = 6$) or activation of RyR with 1 nmol/l ryanodine ($n = 3$) increased cell death in response to SERCA inhibition with 1 μmol/l thapsigargin (Tg). A: ○, control; ▲, 100 μmol/l Cch; ●, 1 μmol/l thapsigargin; ◆, 1 μmol/l thapsigargin + 100 μmol/l Cch. B: ○, control; ●, 1 μmol/l thapsigargin; ◆, 1 μmol/l thapsigargin + 1 nmol/l ryanodine. D and E: MIN6 cells cultured for 8 h with a combination of 100 μmol/l carbachol (Cch) and 1 μmol/l thapsigargin showed increased ER stress (CHOP expression), compared with either treatment alone ($n = 6$). #$P < 0.05$ vs. control; *$P < 0.05$ vs. thapsigargin alone.

pidium iodide incorporation, although this trend did not reach statistical significance (Fig. 4B). The protective effect of dantrolene was also associated with a reduction in the amount of cleaved caspase-3 observed after 8 h of treatment with thapsigargin (Fig. 4C and D). Similarly, the combination of ryanodine and xestospongin C protected cells from thapsigargin-induced caspase-3 cleavage (Fig. 4E–G). The observation that thapsigargin-induced caspase-3 activation, but not total PI incorporation, was significantly reduced by the xestospongin C and ryanodine combination may reflect the fact that PI labeling is not strictly specific for apoptotic death. Thapsigargin-induced CHOP expression at 8 h was also reduced by inhibition of RyRs and IP$_3$Rs (Fig. 4G). Together, these experiments suggest that ER Ca^{2+} release through RyRs and IP$_3$Rs contribute to short-term ER stress and caspase-3–mediated cell death following SERCA inhibition.

In light of these findings, we hypothesized that chronic activation of ER Ca^{2+} release channels might exacerbate the effects of SERCA inhibition. Indeed, thapsigargin-induced cell death was significantly increased when IP$_3$ receptors were concurrently activated

by either 1 μmol/l (not shown) or 100 μmol/l carbachol (Fig. 5A and C). The additional cell death was associated with a dramatic increase in CHOP expression at 8 h (Fig. 5D and E). We further tested this hypothesis using a stimulatory concentration of ryanodine (18,42) and found that 1 nmol/l ryanodine also augmented thapsigargin-induced MIN6 cell death (Fig. 5B and C). Taken together, these data demonstrate that ER Ca^{2+} release channels can both negatively and positively modulate ER stress.

ER Ca^{2+} depletion kinetics and PERK activation in ER stress. Next, we looked for changes in ER luminal Ca^{2+} flux that correlated with the augmentation of β-cell death and ER stress by IP$_3$R activation. Imaging ER Ca^{2+} levels revealed that a combination of thapsigargin and carbachol resulted in a more rapid and homogeneous depletion of ER Ca^{2+} stores, compared with thapsigargin alone (Fig. 6A and B). Following a response to carbachol, the addition of thapsigargin further depleted ER stores (Fig. 6C). When thapsigargin was added first there was a complete depletion and no additional response to carbachol in the majority of cells (Fig. 6D). However, in thapsigargin-treated cells that
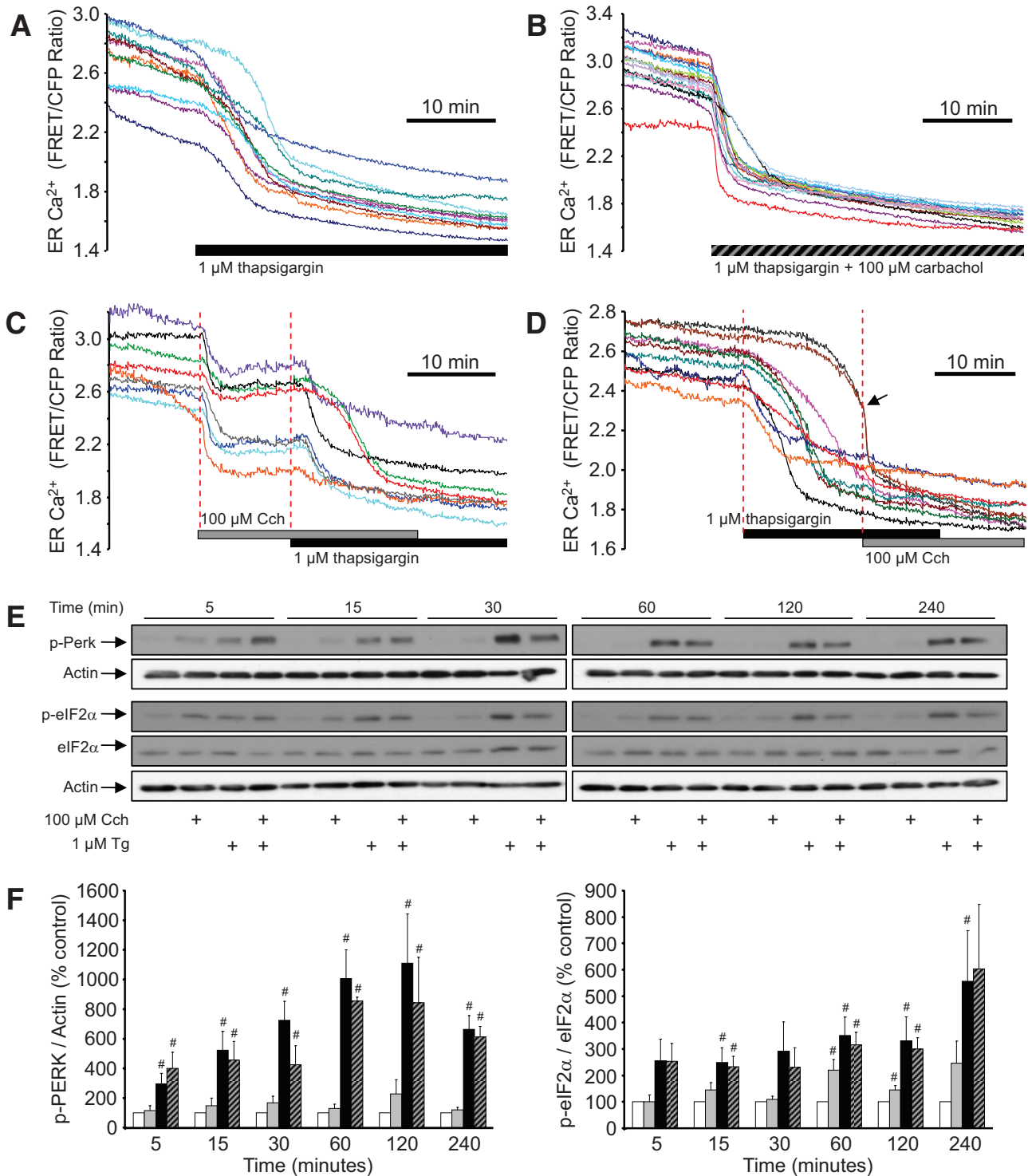
FIG. 6. Effects of IP₃ receptor activation on the ER Ca²⁺ depletion and unfolded protein response activation evoked by SERCA inhibition. *A* and *B*: D1ER cameleon measurements of the luminal ER Ca²⁺ release induced by 1 μmol/l thapsigargin, with or without simultaneous addition of 100 μmol/l carbachol (Cch) (*n* = 10 and 14 cells, respectively). *C*: Effects of 1 μmol/l thapsigargin administered during exposure to 100 μmol/l Cch (*n* = 8 cells). *D*: Effects of 100 μmol/l Cch administered in the presence of 1 μmol/l thapsigargin (*n* = 9 cells). Note the acceleration of ER Ca²⁺ depletion in cells that had not yet reached a stable depleted state (*arrow*). *E*: Phosphorylation of PERK and eIF2α in 25 mmol/l glucose-cultured MIN6 cells was examined at the time points indicated. *F*: Quantification of Western blots for PERK and eIF2α phosphorylation. Similar results from experiments conducted in 5 and 25 mmol/l glucose were pooled (*n* = 6, #*P* < 0.05 vs. control). □, control; ▨ (light gray), 100 μmol/l Cch; ■, 1 μmol/l thapsigargin; ▨, thapsigargin + Cch. (Please see http://dx.doi.org/10.2337/db07-1762 for a high-quality digital representation of this figure).

had not yet fully depleted, carbachol accelerated the ER Ca²⁺ loss (Fig. 6*D*, *arrow*).

What rapid events might link ER Ca²⁺ depletion kinetics to the transcriptional induction of CHOP? Recent work has implicated the eIF2α kinase PERK in the induction of Ca²⁺-dependent ER stress (24). In our experiments, thapsigargin caused sustained PERK and eIF2α phosphorylation that was detectable as early as 5 min (Fig. 6*E* and *F*). There was a tendency for carbachol to augment the thapsigargin-induced phosphorylation of PERK at the
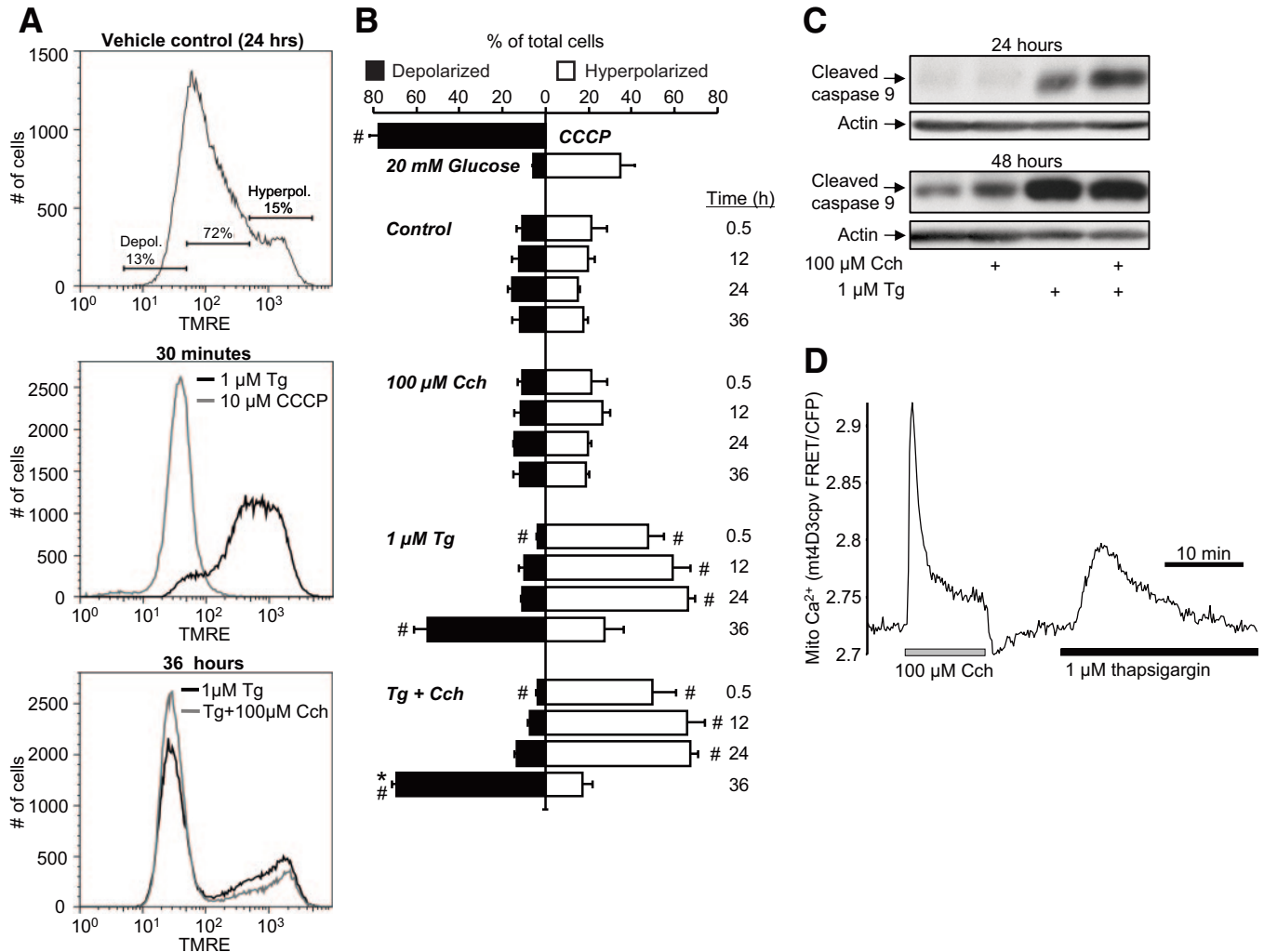
FIG. 7. Time-dependent effects of ER Ca^{2+} depletion on mitochondria. Mitochondrial membrane potential was monitored by flow cytometry analysis of TMRE-stained MIN6 cells. *A*: Representative histograms illustrating that SERCA inhibition rapidly induces mitochondrial hyperpolarization followed later (>24 h) by the collapse of mitochondrial polarization. For quantification, depolarized, intermediate, and hyperpolarized cell populations were defined as indicated in the first panel. CCCP-treated cells are shown as a control for mitochondrial depolarization. *B*: Quantification of the time and treatment dependence of the fraction of cells in the depolarized and hyperpolarized mitochondrial states. (*n* = 12 for CCCP, *n* = 3–4 at each time point for all other treatments; #*P* < 0.05 vs. control at the same time point, *P < 0.05 vs. thapsigargin alone at the same time point.) ■, depolarized; □, hyperpolarized. *C*: Western blots of cleaved caspase-9 levels 24 or 48 h following treatments as indicated. Cleaved caspase-9 normalized to actin (in arbitrary units): 24 h, control 0.42 ± 0.17 vs. 1 µmol/l thapsigargin, 1.01 ± 0.17, *P* < 0.05, *n* = 4; 48 h, control 0.62 ± 0.13 vs. thapsigargin, 2.20 ± 0.48, *P* < 0.05, *n* = 4. *D*: Example of mitochondrial Ca^{2+} responses in a MIN6 cell following mobilization of ER Ca^{2+} by 100 µmol/l carbachol or 1 µmol/l thapsigargin.

5-min time point, potentially linking rapid ER Ca^{2+} depletion to the subsequent amplification of CHOP expression (45). Taken together, these findings suggest that rapid events in the ER lumen can have profound and immediate effects on the unfolded protein response, ER stress, and apoptosis in β-cells.

ER Ca^{2+} depletion evokes multistage perturbations of mitochondrial membrane potential. Evidence indicates that the intrinsic mitochondrial pathway of apoptosis may be triggered during ER stress–associated cell death (46,47). To evaluate the effects on mitochondria, we first analyzed the time-dependent changes in mitochondrial membrane potential by flow cytometry. Interestingly, SERCA inhibition initially caused marked mitochondrial hyperpolarization, suggestive of increased metabolic flux (Fig. 7*A* and *B*). However, mitochondrial polarization ultimately collapsed in the majority of cells, and this depolarization was augmented when IP_3Rs were simultaneously stimulated by carbachol. The activation of mitochondrial apoptosis was further suggested by a significant

increase in cleaved caspase-9 after 24 and 48 h thapsigargin treatment (Fig. 7*C*). Functional cross-talk between ER and mitochondria was evidenced by acute increases in mitochondrial Ca^{2+} following ER Ca^{2+} mobilization by carbachol or thapsigargin (Fig. 7*D*). Together these results provide compelling evidence for the involvement of mitochondria in the regulation and execution of β-cell apoptosis induced by ER Ca^{2+} depletion.

Modulation of ER stress–induced primary mouse islet cell death. We also examined the effects of SERCA and Ca^{2+} channel blockers on dispersed mouse islet cells. Thapsigargin caused progressive dose- and time-dependent death, though it was quantitatively less than what we observed with MIN6 β-cells (Fig. 8*A* and *B*). Nevertheless, carbachol significantly augmented the death of primary cells following SERCA block, in agreement with our MIN6 cell findings. There was also a small degree of cell death in response to carbachol alone (Fig. 8*C*). Combined application of 100 µmol/l ryanodine and 1 µmol/l xestospongin C protected primary β-cells from the potentiating effect of
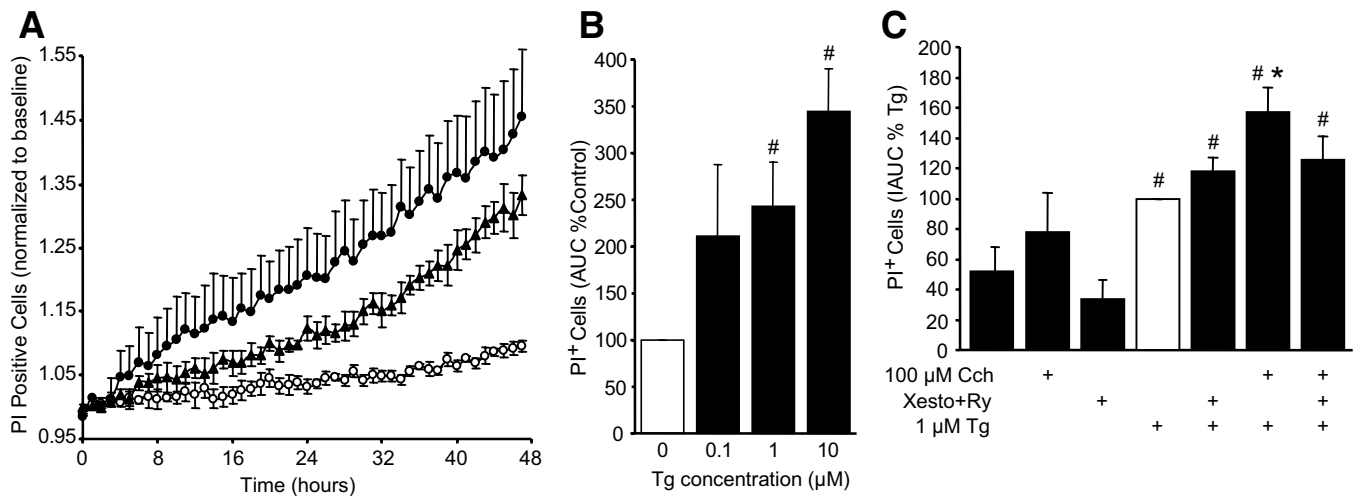
FIG. 8. Effects of SERCA, RyR, and IP$_3$R inhibition on death of primary mouse islet cells. *A*: Representative real-time measurement of the propidium iodide incorporation in primary mouse islet cells exposed to 1 or 10 μmol/l thapsigargin. ○, control; ▲, 1 μmol/l thapsigargin; ●, 10 μmol/l thapsigargin. *B*: Summary of the islet cell death induced by 0.1 μmol/l (*n* = 3), 1 μmol/l (*n* = 5), and 10 μmol/l (*n* = 3) thapsigargin. *C*: Summary of the effects of 100 μmol/l carbachol, 1 μmol/l xestospongin C, and 100 μmol/l ryanodine on the mouse islet cell death induced by 24 h exposure to 1 μmol/l thapsigargin (*n* = 3). #*P* < 0.05 vs. control; *P < 0.05 vs. thapsigargin alone.

carbachol, verifying that it was due to release of intracellular stores. These results suggest that similar, but not identical, mechanisms are involved in MIN6 cell apoptosis and primary β-cell apoptosis in the context of SERCA inhibition.

DISCUSSION

The goal of this study was to determine the specific roles of luminal ER Ca^{2+} influx and efflux mechanisms in the control of β-cell ER stress and apoptosis. To this end, we used a combination of "online" cell death measurements and real-time imaging of ER Ca^{2+} dynamics. First, we determined that blocking ER-resident Ca^{2+} release channels alone was not sufficient to induce substantial ER stress–related cell death. Among the perturbations of β-cell ER Ca^{2+} handling tested, only direct inhibition of SERCA pumps was associated with robust induction of ER stress and activation of caspase-3. Second, we found that thapsigargin-induced apoptosis was attenuated by drugs that reduce channel-mediated Ca^{2+} release from the ER. Third, we established that the effects of thapsigargin on ER Ca^{2+} depletion, ER stress activation, and cell death were accelerated by stimulation of IP$_3$Rs or RyRs. Together, these data provide the first evidence that β-cell ER stress is regulated by the activity of ER-resident Ca^{2+} release channels.

The pathophysiological importance of ER stress and apoptosis in the pancreatic β-cell is becoming increasingly clear (2,5,10). Our identification of conditions that slow and speed up ER stress and cell death elucidates the underlying mechanisms of and may promote strategies for counteracting ER stress associated with cytokines in type 1 diabetes (13), obesity-related type 2 diabetes (10), and rare disorders such as Wolcott-Rallison syndrome and Wolfram's syndrome (5). Indeed, ion channels such as the IP$_3$Rs and RyRs are useful drug targets. The finding that β-cell ER stress might be exacerbated by increased IP$_3$R activity is important because pancreatic β-cells are innervated by cholinergic neurons that likely mobilize ER Ca^{2+} via these channels (48). It is therefore possible that increased nervous tone in the pancreas could aggravate ER stress during the development of diabetes. The expression of type 2 IP$_3$ receptors in β-cells has been shown to be upregulated by chronic hyperglycemia (15), suggesting that β-cell ER stress could also be an indirect complication of diabetes. Given the potential importance of this deleterious positive feedback loop, additional in vivo studies of the role of IP$_3$Rs in ER stress would be valuable.

Little is known about the role of intracellular Ca^{2+} channels in β-cell survival. Recently, we have shown that long-term (>2 days) inhibition of β-cell RyRs activates a programmed cell death pathway that is distinct from the one triggered by SERCA inhibition and instead shares traits with hypoglycemia-induced cell death (17,23). Instead of requiring caspase-3, ryanodine-induced apoptosis requires calpain-10, a human diabetes susceptibility gene (17). In contrast to thapsigargin-induced apoptosis, cell death resulting from RyR inhibition is associated with a decrease in the ATP-to-ADP ratio (23), and increasing the β-cell metabolic rate with high glucose completely abrogates ryanodine-induced programmed cell death (17). For this reason, studies designed to look at the effects of ryanodine on thapsigargin-induced cell death were typically performed in high glucose and on a time scale that precedes the deleterious effects of RyR block (17). Thus, it appears that disruption of β-cell ER Ca^{2+} handling can trigger multiple apoptosis pathways, but only SERCA inhibition leads to robust CHOP induction and caspase-3 activation. The same ER Ca^{2+} pool can thus control several types of cell death, depending in part on whether the filling or release of this pool is disrupted. Our results do not preclude the possibility that intracellular Ca^{2+} channels localized to non-ER compartments, such as insulin granules or endosomes (18,49), might also affect β-cell survival.

The present study provides insight into the complex sequence of events initiated by reduced SERCA activity in β-cells. We demonstrate clear roles for both ER Ca^{2+} levels and mitochondrial membrane potential in ER stress–induced β-cell apoptosis. Our results support that SERCA dysfunction can induce ER stress by rapidly depleting the luminal Ca^{2+} required for proper ER chaperone function and protein folding (11). No difference was observed in the absolute depletion of the ER between cells

treated with thapsigargin alone and thapsigargin plus carbachol. Combined SERCA inhibition and cholinergic activation, however, did result in increased cell death and more rapid and homogeneous depletion kinetics. This suggests that absolute Ca^{2+} levels and the kinetics of luminal Ca^{2+} depletion together dictate the degree of ER stress, perhaps by rapidly modulating PERK phosphorylation. Subsequent to the initial ER-mediated events, there was an early mitochondrial hyperpolarization, in agreement with our previous observation that thapsigargin increased ATP production (23). In agreement with previous work, we found that ER-derived cytosolic Ca^{2+} signals could be sensed by nearby mitochondria (43,50). This might underlie the increased ATP synthesis, as Ca^{2+} in the mitochondrial matrix stimulates respiration via calcium-dependent dehydrogenases (43). On the other hand, excessive mitochondrial Ca^{2+} can trigger the loss of mitochondrial integrity and cell death (9,46,50). We found that β-cell mitochondria eventually fell into a depolarized, "dead" state, but the seemingly transient nature of the thapsigargin-induced Ca^{2+} rise (Fig. 7D) suggests this involves factors other than mitochondrial Ca^{2+} overload or direct ER-mitochondria signaling, per se. However, augmentation of this mitochondrial demise by carbachol indicates some role for Ca^{2+} in this late component of ER stress and CHOP-dependent apoptosis.

In conclusion, we have performed measurements of Ca^{2+} dynamics in the lumens of β-cell organelles, combined with real-time measurements of caspase-3 activation and dynamic assays of β-cell death, to provide a detailed picture of the events mediating β-cell apoptosis associated with disrupted ER Ca^{2+} homeostasis. Our study revealed the involvement of mitochondria in the execution of β-cell ER stress and cell death that results from reduced SERCA activity. Most importantly, we demonstrated a role for the ER Ca^{2+} release channels in the regulation of this important β-cell ER stress and apoptosis pathway. Together, these observations provide new insight into the mechanisms by which β-cells die in diabetes, knowledge that is essential for therapeutic efforts to reduce β-cell death.

REFERENCES

1. Harding HP, Ron D: Endoplasmic reticulum stress and the development of diabetes: a review. *Diabetes* 51 (Suppl. 3):S455–S461, 2002
2. Huang CJ, Lin CY, Haataja L, Gurlo T, Butler AE, Rizza RA, Butler PC: High expression rates of human islet amyloid polypeptide induce endoplasmic reticulum stress–mediated β-cell apoptosis, a characteristic of humans with type 2 but not type 1 diabetes. *Diabetes* 56:2016–2027, 2007
3. Cnop M, Welsh N, Jonas JC, Jorns A, Lenzen S, Eizirik DL: Mechanisms of pancreatic β-cell death in type 1 and type 2 diabetes: many differences, few similarities. *Diabetes* 54 (Suppl. 2):S97–S107, 2005
4. Johnson JD, Ahmed NT, Luciani DS, Han Z, Tran H, Fujita J, Misler S, Edlund H, Polonsky KS: Increased islet apoptosis in Pdx1$^{+/-}$ mice. *J Clin Invest* 111:1147–1160, 2003
5. Yamada T, Ishihara H, Tamura A, Takahashi R, Yamaguchi S, Takei D, Tokita A, Satake C, Tashiro F, Katagiri H, Aburatani H, Miyazaki J, Oka Y: WFS1-deficiency increases endoplasmic reticulum stress, impairs cell cycle progression and triggers the apoptotic pathway specifically in pancreatic β-cells. *Hum Mol Genet* 15:1600–1609, 2006
6. Davalli AM, Scaglia L, Zangen DH, Hollister J, Bonner-Weir S, Weir GC: Vulnerability of islets in the immediate posttransplantation period: dynamic changes in structure and function. *Diabetes* 45:1161–1167, 1996
7. Orrenius S, Zhivotovsky B, Nicotera P: Regulation of cell death: the calcium-apoptosis link. *Nat Rev Mol Cell Biol* 4:552–565, 2003
8. Oyadomari S, Araki E, Mori M: Endoplasmic reticulum stress-mediated apoptosis in pancreatic β-cells. *Apoptosis* 7:335–345, 2002
9. Hajnoczky G, Csordas G, Madesh M, Pacher P: Control of apoptosis by IP(3) and ryanodine receptor driven calcium signals. *Cell Calcium* 28:349–363, 2000
10. Ozcan U, Cao Q, Yilmaz E, Lee AH, Iwakoshi NN, Ozdelen E, Tuncman G, Gorgun C, Glimcher LH, Hotamisligil GS: Endoplasmic reticulum stress links obesity, insulin action, and type 2 diabetes. *Science* 306:457–461, 2004
11. Michalak M, Robert Parker JM, Opas M: Ca^{2+} signaling and calcium binding chaperones of the endoplasmic reticulum. *Cell Calcium* 32:269–278, 2002
12. Zhou YP, Teng D, Dralyuk F, Ostrega D, Roe MW, Philipson L, Polonsky KS: Apoptosis in insulin-secreting cells: evidence for the role of intracellular Ca^{2+} stores and arachidonic acid metabolism. *J Clin Invest* 101:1623–1632, 1998
13. Cardozo AK, Ortis F, Storling J, Feng YM, Rasschaert J, Tonnesen M, Van Eylen F, Mandrup-Poulsen T, Herchuelz A, Eizirik DL: Cytokines downregulate the sarcoendoplasmic reticulum pump Ca^{2+} ATPase 2b and deplete endoplasmic reticulum Ca^{2+}, leading to induction of endoplasmic reticulum stress in pancreatic β-cells. *Diabetes* 54:452–461, 2005
14. Varadi A, Molnar E, Ostenson CG, Ashcroft SJ: Isoforms of endoplasmic reticulum Ca^{2+}-ATPase are differentially expressed in normal and diabetic islets of Langerhans. *Biochem J* 319:521–527, 1996
15. Lee B, Jonas JC, Weir GC, Laychock SG: Glucose regulates expression of inositol 1,4,5-trisphosphate receptor isoforms in isolated rat pancreatic islets. *Endocrinology* 140:2173–2182, 1999
16. Islam MS, Leibiger I, Leibiger B, Rossi D, Sorrentino V, Ekstrom TJ, Westerblad H, Andrade FH, Berggren PO: In situ activation of the type 2 ryanodine receptor in pancreatic β cells requires cAMP-dependent phosphorylation. *Proc Natl Acad Sci U S A* 95:6145–6150, 1998
17. Johnson JD, Han Z, Otani K, Ye H, Zhang Y, Wu H, Horikawa Y, Misler S, Bell GI, Polonsky KS: RyR2 and calpain-10 delineate a novel apoptosis pathway in pancreatic islets. *J Biol Chem* 279:24794–24802, 2004
18. Johnson JD, Kuang S, Misler S, Polonsky KS: Ryanodine receptors in human pancreatic β cells: localization and effects on insulin secretion. *FASEB J* 18:878–880, 2004
19. Chen L, Koh DS, Hille B: Dynamics of calcium clearance in mouse pancreatic β-cells. *Diabetes* 52:1723–1731, 2003
20. Bidasee KR, Nallani K, Henry B, Dincer UD, Besch HR Jr: Chronic diabetes alters function and expression of ryanodine receptor calcium-release channels in rat hearts. *Mol Cell Biochem* 249:113–123, 2003
21. Sharma K, Wang L, Zhu Y, DeGuzman A, Cao GY, Lynn RB, Joseph SK: Renal type I inositol 1,4,5-trisphosphate receptor is reduced in streptozotocin-induced diabetic rats and mice. *Am J Physiol* 276:F54–F61, 1999
22. Srivastava M, Eidelman O, Leighton X, Glasman M, Goping G, Pollard HB: Anx7 is required for nutritional control of gene expression in mouse pancreatic islets of Langerhans. *Mol Med* 8:781–797, 2002
23. Dror V, Kalynyak TB, Bychkivska Y, Frey MH, Tee M, Jeffrey KD, Nguyen V, Luciani DS, Johnson JD: Glucose and endoplasmic reticulum calcium channels regulate HIF-1β via presenilin in pancreatic β-cells. *J Biol Chem* 283:9909–9916, 2008
24. Liang SH, Zhang W, McGrath BC, Zhang P, Cavener DR: PERK (eIF2α kinase) is required to activate the stress-activated MAPKs and induce the expression of immediate-early genes upon disruption of ER calcium homoeostasis. *Biochem J* 393:201–209, 2006
25. Gomez E, Powell ML, Bevington A, Herbert TP: A decrease in cellular energy status stimulates PERK-dependent eIF2α phosphorylation and regulates protein synthesis in pancreatic β-cells. *Biochem J* 410:485–493, 2008
26. Li F, Hayashi T, Jin G, Deguchi K, Nagotani S, Nagano I, Shoji M, Chan PH, Abe K: The protective effect of dantrolene on ischemic neuronal cell death is associated with reduced expression of endoplasmic reticulum stress markers. *Brain Res* 1048:59–68, 2005

27. Hoyer-Hansen M, Jaattela M: Connecting endoplasmic reticulum stress to autophagy by unfolded protein response and calcium. *Cell Death Differ* 14:1576–1582, 2007

28. Johnson JD, Ford EL, Bernal-Mizrachi E, Kusser KL, Luciani DS, Han Z, Tran H, Randall TD, Lund FE, Polonsky KS: Suppressed insulin signaling and increased apoptosis in CD38-null islets. *Diabetes* 55:2737–2746, 2006

29. Salvalaggio PR, Deng S, Ariyan CE, Millet I, Zawalich WS, Basadonna GP, Rothstein DM: Islet filtration: a simple and rapid new purification procedure that avoids ficoll and improves islet mass and function. *Transplantation* 74:877–879, 2002

30. Luciani DS, Ao P, Hu X, Warnock GL, Johnson JD: Voltage-gated Ca²⁺ influx and insulin secretion in human and mouse β-cells are impaired by the mitochondrial Na⁺/Ca²⁺ exchange inhibitor CGP-37157. *Eur J Pharmacol* 576:18–25, 2007

31. Palmer AE, Jin C, Reed JC, Tsien RY: Bcl-2-mediated alterations in endoplasmic reticulum Ca²⁺ analyzed with an improved genetically encoded fluorescent sensor. *Proc Natl Acad Sci U S A* 101:17404–17409, 2004

32. Palmer AE, Giacomello M, Kortemme T, Hires SA, Lev-Ram V, Baker D, Tsien RY: Ca²⁺ indicators based on computationally redesigned calmodulin-peptide pairs. *Chem Biol* 13:521–530, 2006

33. Karasawa S, Araki T, Nagai T, Mizuno H, Miyawaki A: Cyan-emitting and orange-emitting fluorescent proteins as a donor/acceptor pair for fluorescence resonance energy transfer. *Biochem J* 381:307–312, 2004

34. Smolewski P, Grabarek J, Halicka HD, Darzynkiewicz Z: Assay of caspase activation in situ combined with probing plasma membrane integrity to detect three distinct stages of apoptosis. *J Immunol Methods* 265:111–121, 2002

35. Gottlieb E, Vander Heiden MG, Thompson CB: Bcl-x(L) prevents the initial decrease in mitochondrial membrane potential and subsequent reactive oxygen species production during tumor necrosis factor α-induced apoptosis. *Mol Cell Biol* 20:5680–5689, 2000

36. Varadi A, Rutter GA: Dynamic imaging of endoplasmic reticulum Ca²⁺ concentration in insulin-secreting MIN6 cells using recombinant targeted cameleons: roles of sarco(endo)plasmic reticulum Ca²⁺-ATPase (SERCA)-2 and ryanodine receptors. *Diabetes* 51 (Suppl. 1):S190–S201, 2002

37. Gylfe E: Carbachol induces sustained glucose-dependent oscillations of cytoplasmic Ca2+ in hyperpolarized pancreatic beta cells. *Pflugers Arch* 419:639–643, 1991

38. Dyachok O, Gylfe E: Store-operated influx of Ca²⁺ in pancreatic β-cells exhibits graded dependence on the filling of the endoplasmic reticulum. *J Cell Sci* 114:2179–2186, 2001

39. Liou J, Fivaz M, Inoue T, Meyer T: Live-cell imaging reveals sequential oligomerization and local plasma membrane targeting of stromal interaction molecule 1 after Ca²⁺ store depletion. *Proc Natl Acad Sci U S A* 104:9301–9306, 2007

40. Oyadomari S, Koizumi A, Takeda K, Gotoh T, Akira S, Araki E, Mori M: Targeted disruption of the Chop gene delays endoplasmic reticulum stress-mediated diabetes. *J Clin Invest* 109:525–532, 2002

41. Bilmen JG, Wootton LL, Godfrey RE, Smart OS, Michelangeli F: Inhibition of SERCA Ca²⁺ pumps by 2-aminoethoxydiphenyl borate (2-APB). 2-APB reduces both Ca²⁺ binding and phosphoryl transfer from ATP, by interfering with the pathway leading to the Ca²⁺-binding sites. *Eur J Biochem* 269:3678–3687, 2002

42. Johnson JD, Misler S: Nicotinic acid-adenine dinucleotide phosphate-sensitive calcium stores initiate insulin signaling in human beta cells. *Proc Natl Acad Sci U S A* 99:14566–14571, 2002

43. Tsuboi T, da Silva Xavier G, Holz GG, Jouaville LS, Thomas AP, Rutter GA: Glucagon-like peptide-1 mobilizes intracellular Ca²⁺ and stimulates mitochondrial ATP synthesis in pancreatic MIN6 β-cells. *Biochem J* 369:287–299, 2003

44. Malli R, Frieden M, Trenker M, Graier WF: The role of mitochondria for Ca²⁺ refilling of the endoplasmic reticulum. *J Biol Chem* 280:12114–12122, 2005

45. Ma Y, Brewer JW, Diehl JA, Hendershot LM: Two distinct stress signaling pathways converge upon the CHOP promoter during the mammalian unfolded protein response. *J Mol Biol* 318:1351–1365, 2002

46. Deniaud A, Sharaf el dein O, Maillier E, Poncet D, Kroemer G, Lemaire C, Brenner C: Endoplasmic reticulum stress induces calcium-dependent permeability transition, mitochondrial outer membrane permeabilization and apoptosis. *Oncogene* 27:285–299, 2008

47. Masud A, Mohapatra A, Lakhani SA, Ferrandino A, Hakem R, Flavell RA: Endoplasmic reticulum stress-induced death of mouse embryonic fibroblasts requires the intrinsic pathway of apoptosis. *J Biol Chem* 282:14132–14139, 2007

48. Gilon P, Henquin JC: Mechanisms and physiological significance of the cholinergic control of pancreatic β-cell function. *Endocr Rev* 22:565–604, 2001

49. Mitchell KJ, Pinton P, Varadi A, Tacchetti C, Ainscow EK, Pozzan T, Rizzuto R, Rutter GA: Dense core secretory vesicles revealed as a dynamic Ca²⁺ store in neuroendocrine cells with a vesicle-associated membrane protein aequorin chimaera. *J Cell Biol* 155:41–51, 2001

50. Filippin L, Magalhaes PJ, Di Benedetto G, Colella M, Pozzan T: Stable interactions between mitochondria and endoplasmic reticulum allow rapid accumulation of calcium in a subpopulation of mitochondria. *J Biol Chem* 278:39224–39234, 2003